Percolative Conduction in the Half-Metallic-Ferromagnetic and Ferroelectric Mixture of (La, Lu, Sr)MnO_3

S. Park, N. Hur, S. Guha, and S.-W. Cheong

Department of Physics & Astronomy, Rutgers University, Piscataway, New Jersey 08854, USA

(Received 22 May 2003; published 23 April 2004)

The *immiscibility* between rhombohedral $La_{5/8}Sr_{3/8}MnO_3$ and hexagonal $LuMnO_3$ leads to a μm-scale heterogeneous mixture of half-metallic-ferromagnetic and insulating-ferroelectric phases. Electronic conduction of the mixture exhibits nearly ideal percolation behavior in the paramagnetic state with a threshold of 0.224(5) metal volume fraction and a resistivity scaling exponent $t = 2.1 \pm 0.1$, consistent with the predicted universal behavior of classical percolation. However, far below T_C, t increases to 2.4 ± 0.1, probably resulting from intergrain tunneling. Therefore, this system represents a unique example of the temperature-induced crossover from *universal* to *nonuniversal* behavior of t.

DOI: 10.1103/PhysRevLett.92.167206 PACS numbers: 75.47.Lx, 72.60.+g, 75.50.Cc, 77.80.–e

There has been significant interest in multiferroic materials, which simultaneously exhibit (anti)ferromagnetism (FM) and (anti)ferroelectricity (FE). However, only a limited number of chemical compounds have been found to be multiferroic and, correspondingly, the understanding of this rare phenomenon has been of great scientific concern. In addition, the ability to control the intricate interplay between magnetic and dielectric properties in multiferroics may lead to a variety of future technological applications such as magnetic-field-tunable microwave devices [1].

The manganese perovskites, $AMnO_3$ with A being rare earths or alkali earth metals, crystallize in two structural phases: a cubic-related phase and a hexagonal phase. It turns out that the structure is primarily determined by the size of A-site ions. For example, $LaMnO_3$ is orthorhombic, but the small rare earth in $YMnO_3$ (YMO) or $LuMnO_3$ (LMO) stabilizes the hexagonal structure. In addition to this structural variety, the manganese perovskites display a wide range of physical properties such as FM in Sr-doped $LaMnO_3$ and FE in YMO or LMO [2–4].

$La_{5/8}Sr_{3/8}MnO_3$ (LSMO) crystallizes in the rhombohedral structure with an optimal Curie temperature (T_C) of 370 K. The Néel temperature (T_N) and FE transition temperature (T) of hexagonal LMO are 90 K and about 900 K, respectively. While investigating the doping effect of small Lu ions to LSMO, we have, unexpectedly, discovered that an almost-complete *chemical immiscibility* exists between FM-metallic (M) LSMO and FE-insulating (I) LMO. Therefore, this is an ideal system in which to study percolative electronic transport in a mixture of FM and FE phases.

Percolative properties of composite materials have been studied theoretically as well as experimentally for a number of decades [5,6]. Experimental examples include the mixture of SiO_2 and FM Ni, where the spin degree of freedom has important consequences for percolative conduction [7]. In this Letter, we present detailed structural, magnetic, and electronic transport studies of the phase-separated mixture (x)LSMO:$(1-x)$LMO. It is noteworthy that the FM LSMO is half-M, i.e., all the charge carriers are completely spin polarized when FM is fully developed [8,9].

Polycrystalline (x)LSMO:$(1-x)$LMO specimens with about 20 different molar ratios were prepared through conventional solid-state reaction in air. The samples were sintered at 1300–1400 °C for 48 h with intermediate grindings, followed by annealing in an oxygen environment. Resistivity (ρ) was measured by using the standard four-probe method, and a SQUID magnetometer was used for magnetization measurement.

X-ray powder diffraction results on (x)LSMO:$(1-x)$LMO in Fig. 1(a) clearly demonstrate chemical phase separation. Mixed specimens show both rhombohedral and hexagonal diffraction patterns. While the diffraction peak positions have a negligible shift with varying composition, the relative intensities of the two peaks systematically change with x. This observation is rather surprising in the sense that an almost-complete immiscibility exists within a mixture of two compounds having a nearly identical chemical formula, $AMnO_3$. We found that in other mixtures such as LSMO/hexagonal $YMnO_3$ and LSMO/orthorhombic $DyMnO_3$, the solubility limits are approximately 10% and 20%, respectively, judging from the lattice parameter shift. This rather unique property of LSMO:LMO may stem from the extreme difference between the ionic radius of La and Lu.

Polarized optical microscopy directly reveals the μm-scale phase separation in 0.3LSMO:0.7LMO [Figs. 1(b) and 1(c)]. LSMO grains can be readily identified in unpolarized images such as Fig. 1(b), due to their lower reflectivity in the visible range. Correspondingly, grain 5 is identified to be LSMO, and grains 1–4 are LMO. Now, a significant optical anisotropy exists in hexagonal LMO due to the optical difference between the a/b and the c axis. In contrast, LSMO is nearly

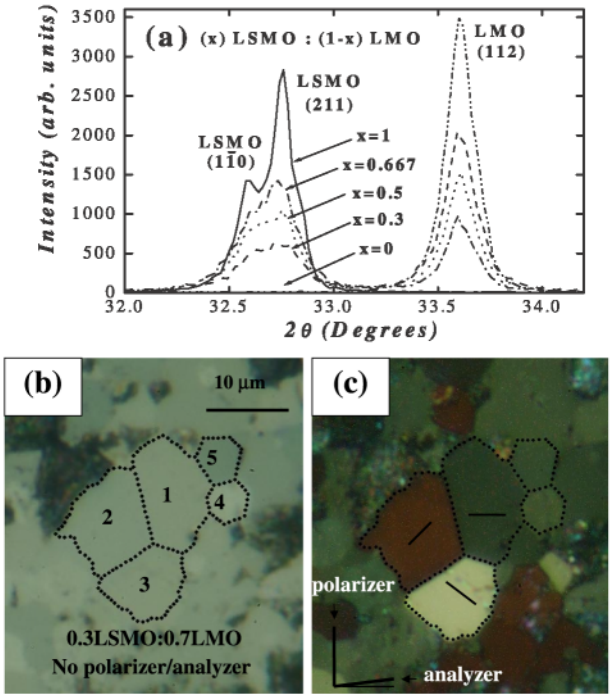

FIG. 1 (color online). (a) Powder x-ray diffraction intensity vs 2θ for (x)LSMO:$(1-x)$LMO. The $(1\bar{1}0)$ and (211) peaks of LSMO and the (112) peak of LMO are denoted. (b) Unpolarized optical microscope image of (x)LSMO:$(1-x)$LMO with $x = 0.3$. Grains 1–3 are LMO with a c-axis component, grain 4 is LMO in the a-b plane, and grain 5 is LSMO. (c) Polarized image: polarizer and analyzer angles are also depicted and lines in three grains show the c-axis orientation of LMO.

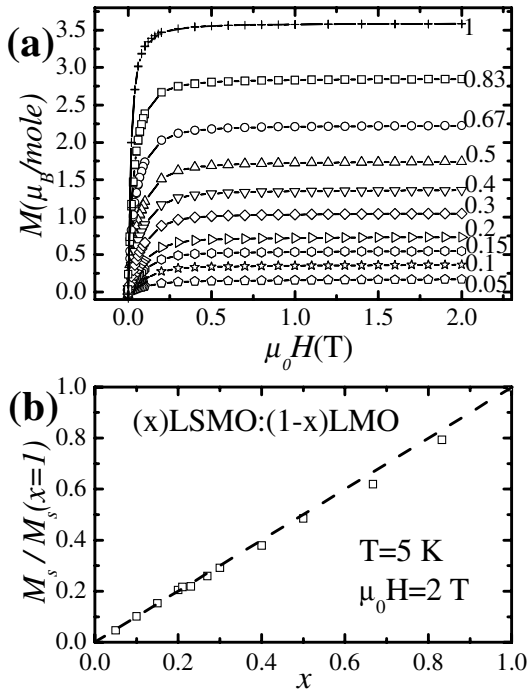

FIG. 2. (a) Magnetization curves of (x)LSMO:$(1-x)$LMO vs external fields up to 2 T at 5 K. (b) Saturation magnetic moment per Mn vs metallic molar ratio x (LSMO). The dashed lines are to guide the eyes.

optically isotropic since it possesses only a slight rhombohedral distortion away from cubic symmetry. This optical anisotropy can be utilized to identify the orientation of the c axis by observing the change of contrast/color with the variation of angle between a polarizer and an analyzer as well as the angle between the sample and the polarizer. For example, in Fig. 1(c), taken with a polarizer and an analyzer (having an angle slightly less than 90° to each other), the brightest contrast was observed when the c-axis component of a LMO grain 3 was located at about $-45°$ with respect to the polarizer. The c-axis orientations identified in this way are depicted for grains 1–3 in Fig. 1(c). The surface of grain 4 turns out to be along the ab plane. This figure shows a grain size of about 10 μm for LMO and 5 μm for LSMO. The relatively larger grain size of LMO probably results from its lower melting T compared to LSMO. This causes a fast grain growth of LMO at a fixed sintering T ($\sim$1300 °C).

To understand the magnetic nature of this phase-separated mixtures LSMO:LMO, we have measured the external field (H) dependent magnetization at 5 K as shown in Fig. 2(a). As evident in Fig. 2(b), near $x = 0$ (LMO) the saturated FM moments (M_S) all fall on a straight line, but $x = 0.4$–0.833 show only a slight deviation from linearity. We speculate that this deviation may arise from a small manganese/oxygen deficiency. Nevertheless, the behavior of the magnetization attests the phase separation of LSMO:LMO.

Percolative conduction in this μm-scale mixture is naturally expected from the above results. Increasing the amount of LMO systematically increases ρ until a M-I transition occurs between $x = 0.22$ and 0.23 as shown in Figs. 3(a) and 3(b). Note that $\rho(T)$ retains the almost identical metallic T dependence of LSMO down to $x = 0.25$, despite an increase of 4 orders of magnitude in the absolute value. This results from the reduced cross sectional area of conducting paths as the I volume fraction is increased. A similar trend in ρ has been shown in microscopic-scale electronic phase mixtures, such as $La_{5/8\text{-}y}Pr_yCa_{3/8}MnO_3$ [10] and $Mg_{1-x}B_2$ [11]. $La_{5/8\text{-}y}Pr_yCa_{3/8}MnO_3$ phase-separates into a FM-M and charge ordered-I mixture at low T, while $Mg_{1-x}B_2$ is composed of a mixture of superconducting M and disorder-induced I phases.

We can obtain a better understanding of the solubility of the different phases by monitoring T_C for each mixture, determined by the peak position of $d\rho/dT$. While T_C initially decreased from 372 K for $x = 1$ (optimally doped LSMO) to 357 K for $x = 0.985$, there was no significant shift for all lower x composites as shown in Fig. 4(b). The solubility of LMO into LSMO is therefore about 1%. This is in stark contrast to the LSMO:YMO

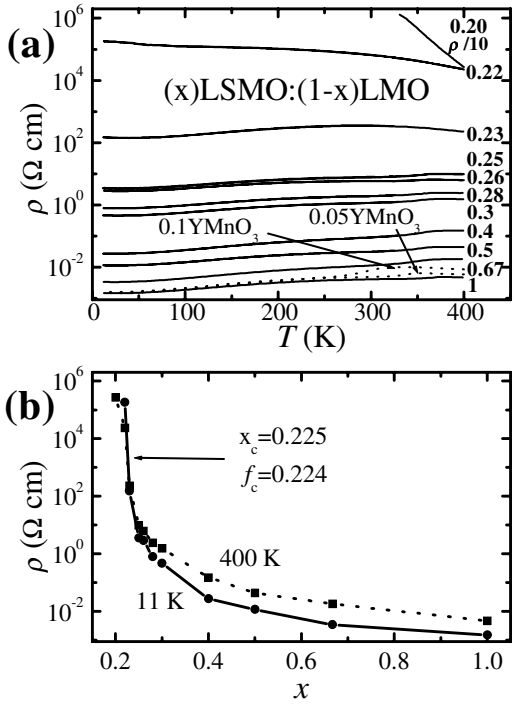

FIG. 3. (a) Resistivity of (x)LSMO:$(1-x)$LMO as a function of temperature for various metallic *molar* ratios, x. Dotted lines represent LSMO:$YMnO_3$. (b) Resistivity at 400 and 11 K as a function of x. f represents metallic *volume* ratios, and percolation threshold is chosen as $f_c = 0.224$, corresponding to $x_c = 0.225$.

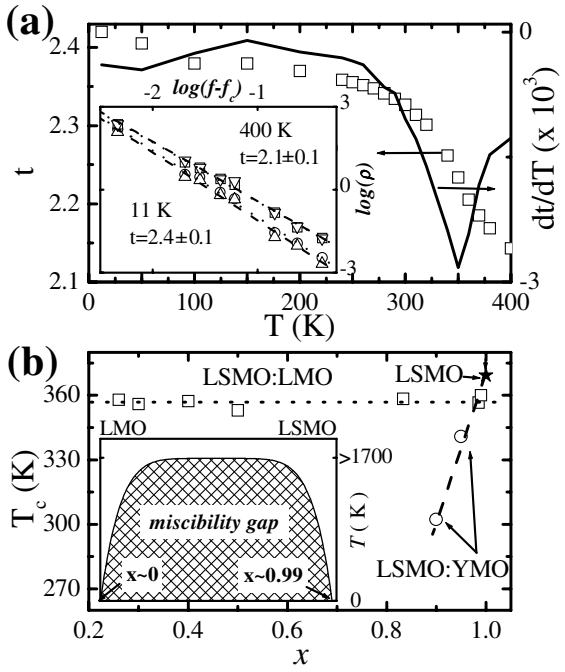

FIG. 4. (a) The resistivity exponent, t, as a function of temperature. The solid line represents the temperature derivative of t, demonstrating its correlation to the FM T_C (~355 K) of the system. The inset shows $\log(\rho)$ vs $\log(f - f_c)$ at 11 and 400 K. (b) FM T_C as a function of x. The inset shows a schematic phase diagram of (x)LSMO:$(1-x)$LMO.

mixture. The T_C of LSMO:YMO sharply decreases to ~340 and ~300 K with the introduction of 5% and 10% YMO, respectively. A schematic phase diagram, inferred from Fig. 4(b), is depicted in the inset of the figure. Evidently, the *miscibility gap* of LSMO:LMO is quite large, between ~0% and ~99%. Note that there was no change in T_N for LMO, which becomes antiferromagnetic at ~90 K, indicating the negligible solubility of LSMO into LMO. The upper limit of solubility is shown at $T > 1700$ K to indicate that a single phase is not formed within the sintering T region.

The *immiscibility* between LSMO and LMO allows the study of detailed percolative conduction in a FM-FE mixture. As shown in Fig. 3(b) as well as the inset of Fig. 4(a), the resistivity was found to obey the scaling law $\rho \propto (f - f_c)^{-t}$ in the entire M compositional range, where f is the M volume ratio, f_c is the percolation threshold of the M phase, and t is the resistivity exponent [5]. Note that f_c is 0.224(5) for $x_c = 0.225(5)$ [12], which falls in the range of the theoretical predictions of three-dimensional (3D) continuum percolation models. In these models, the threshold is reported to be $f_c = 0.29$ when the M volume was permitted to overlap, and 0.15 if overlapping is prohibited [13]. At 400 K, the exponent t was 2.1 ± 0.1, in good agreement with the predicted universal value of $t = 2.0$ for 3D percolative conduction [6]. This observation indicates that at high T above T_C, the electronic conduction in LSMO:LMO follows the classical 3D continuum model, where permeable M particles carry the current. Note that 1 tesla H had no influence on t as expected from the paramagnetic characteristic at 400 K.

However, we found that t increases to 2.4 ± 0.1 with negligible H dependence at 11 K. It has been well established that, for polycrystalline LSMO specimens at low T (far below FM T_C), intergrain spin-polarized tunneling is the dominant contribution to ρ, which is significantly larger than that of single crystals without grain boundaries. This difference becomes negligible at high T above T_C [8]. It turns out that the intergrain tunneling is responsible for the observed ~33% low T magnetoresistance in low fields in polycrystalline LSMO [9]. Note that this intergrain tunneling is intricately coupled with the half-M nature of double-exchange LSMO. Interestingly, for all of our LSMO:LMO specimens in the M region, the T dependence of ρ as well as the magnitude of the low field magnetoresistance (~30% at 11 K) are quite similar to those of polycrystalline LSMO. An additional indication for tunneling transport in our system is the *weak* T dependence of ρ for $x = 0.22$ in Fig. 3(a), which is in the I region [14]. Therefore, intergrain tunneling appears to determine the magnitude of ρ at low T in our mixed system. Chen *et al.* have reported a resistivity

scaling exponent $t = 2.3$, which is close to our value, for carbon particles embedded in an I organic, where the conduction mechanism is known to be of the tunneling type [15]. Furthermore, Balberg has shown that interparticle tunneling, contrary to the classical "touching particles" model, can yield a nonuniversal behavior of the critical exponent, including an increase in t from the universal value of $t = 2.0$ [16]. Therefore, it is rather conclusive that the small, but clear increase of t in our system originates from the nonuniversal behavior of t for intergrain tunneling at low T. Note that a $\sim$30% change of ρ is negligible in the logarithmic scale, corroborating the negligible change of t in H at low T. We also point out that the overall temperature dependence of t, depicted in Fig. 4(a), shows a sudden change of t near FM T_C, consistent with the picture that the crossover from universal to nonuniversal behavior of t is associated with spin-dependent tunneling between FM grains

Another intriguing feature of our results is that ρ obeys the same scaling law far to the M end ($x \approx 0.99$), which appears to be odd in the sense that critical behavior may be valid only very near f_c. However, our experimental observation is consistent with the theoretical prediction of the generalized conductivity for 3D site percolation [13]. For example, Adler *et al.* have shown that ρ obeys a power law with $t = 2$ not only just above f_c but also over the entire M range of $f_c \leq f \leq 1$ from both numerical and experimental simulations of the 3D cubic lattice [17]. The wide range of M volume fractions over which we have observed the scaling relation to hold suggests site percolation is an important consideration.

In summary, we have made the unprecedented discovery of the *immiscibility* between a half-M FM and a FE, resulting in a new kind of multiferroics with a composite character. In this phase-separated system, the percolative M-I transition occurs at $f_c = 0.224(5)$. Above the FM T_C, $t = 2.1 \pm 0.1$, in good agreement with the predicted universal behavior ($t = 2.0$) of classical percolation. However, far below T_C the exponent changes to 2.4 ± 0.1. This crossover to a nonuniversal behavior at low T originates from the change of the primary conduction mechanism in the M/I mixture. In the paramagnetic state, the network configuration of M domains dominates the overall conduction, but at low T, where FM half-M is fully developed, conduction is instead determined by the tunneling across M grain boundaries, which has been predicted to produce nonuniversality.

We thank P. A. Sharma for valuable comments on this Letter. This work was supported by the National Science Foundation under Grant No. 0103858.

[1] J. Wang, J. B. Neaton, H. Zheng, V. Nagarajan, S. B. Ogale, B. Liu, D. Viehland, V. Vaithyanathan, D. G. Schlom, U. V. Waghmare, N. A. Spaldin, K. M. Rabe, M. Wuttig, and R. Ramesh, Science **299**, 1719 (2003).
[2] K. Ghosh, C. J. Lobb, R. L. Greene, S. G. Karabashev, D. A. Shulyatev, A. A. Arsenov, and Y. Mukovskii, Phys. Rev. Lett. **81**, 4740 (1998).
[3] B. B. Van Aken, Jan-Willem G. Bos, R. A. de Groot, and T. T. M. Palstra, Phys. Rev. B **63**, 125127 (2001).
[4] T. Katsufuji, S. Mori, M. Masaki, Y. Moritomo, N. Yamamoto, and H. Takagi, Phys. Rev. B **64**, 104419 (2001).
[5] B. I. Shklovskii and A. L. Efros, *Electronic Properties of Doped Semiconductors* (Springer, New York, 1984).
[6] M. Sahimi, *Application of Percolation Theory* (Taylor & Francis, London, 1994).
[7] J. S. Helman and B. Abeles, Phys. Rev. Lett. **37**, 1429 (1976).
[8] H. Y. Hwang, S.-W. Cheong, N. P. Ong, and B. Batlogg, Phys. Rev. Lett. **77**, 2041 (1996).
[9] S. Lee, H. Y. Hwang, B. I. Shraiman, W. D. Ratcliff II, and S.-W. Cheong, Phys. Rev. Lett. **82**, 4508 (1999).
[10] L. Zhang, C. Israel, A. Biswas, R. L. Greene, and A. Lozanne, Science **298**, 805 (2002).
[11] P. A. Sharma, N. Hur, Y. Horibe, C. H. Chen, B. G. Kim, S. Guha, M. Z. Cieplak, and S.-W. Cheong, Phys. Rev. Lett. **89**, 167003 (2002).
[12] f is calculated from the molar ratio, x, by using the unit cell densities of each parent compound with the assumption that only 1% of LMO is soluble into LSMO. As evident in Fig. 3(b), f_c lies within 0.22 and 0.23. The exact value of $f_c = 0.224(5)$ is determined by requiring the linearity of the data in the inset of Fig. 4(a), and the magnitude of t is estimated from a least-squares linear fit. This result is consistent with the result of a multiple parameter fitting.
[13] S. Kirkpatrick, Rev. Mod. Phys. **45**, 574 (1973).
[14] J. J. Åkerman, J. M. Slaughter, R. W. Dave, and I K. Schuller, Appl. Phys. Lett. **79**, 3104 (2001).
[15] C. C. Chen and Y. C. Chou, Phys. Rev. Lett. **54**, 2529 (1985).
[16] I. Balberg, Phys. Rev. Lett. **59**, 1305 (1987).
[17] D. Adler, L. P. Flora, and S. D. Senturia, Solid State Commun. **12**, 9 (1973).